

IAM: Efficient Inference through Attention Mapping between Different-scale LLMs

Anonymous ACL submission

Abstract

LLMs encounter significant challenges in resource consumption nowadays, especially with long contexts. Despite extensive efforts dedicated to enhancing inference efficiency, these methods primarily exploit internal sparsity within the models, without leveraging external information for optimization. We identify the high similarity of attention matrices across different-scale LLMs, which offers a novel perspective for optimization. We first conduct a comprehensive analysis of how to measure similarity, how to select mapping Layers and whether mapping is consistency. Based on these insights, we introduce the IAM framework, which achieves dual benefits of accelerated attention computation and reduced KV cache usage by performing attention mapping between small and large LLMs. Our experimental results demonstrate that IAM can accelerate prefill by 15% and reduce KV cache usage by 22.1% without appreciably sacrificing performance. Experiments on different series of models show the generalizability of IAM. Importantly, it is also orthogonal to many existing KV cache optimization methods, making it a versatile addition to the current toolkit for enhancing LLM efficiency.

1 Introduction

Large language models (LLMs) like GPT4 (OpenAI, 2024a) have emerged with remarkable natural language understanding capabilities and broad prospects in application. Subsequent advancements such as In-Context Learning (ICL) (Brown, 2020; Dong et al., 2024), Chain-of-Thought (CoT) (Wei et al., 2022; Yao et al., 2024) and Retrieval Augmented Generation (RAG) (Lewis et al., 2020) have significantly revitalized the landscape of applications based on LLMs. These technologies expand the capabilities of LLMs by enabling the activation of domain-specific knowledge or strengthening memory capabilities. However, they also in-

troduce significant computation and memory consumption due to exceedingly long contexts. Recent developments in reasoning models, exemplified by ChatGPT-o1 (OpenAI, 2024b) and DeepSeek-R1 (DeepSeek-AI, 2025), have exacerbated this issue because of their extensive internal reasoning processes.

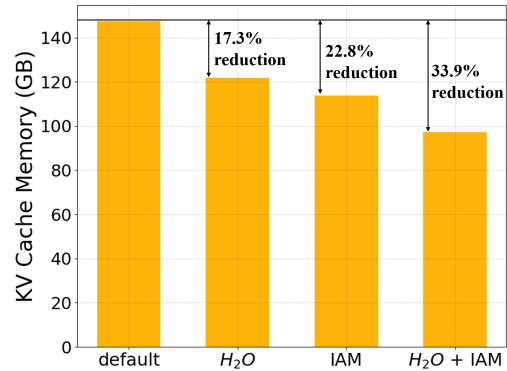


Figure 1: IAM is orthogonal to the existing KV cache eviction methods and can further reduce the KV cache usage in long context scenarios.

To address the aforementioned challenges and achieve efficient inference, various methodologies have been proposed, including optimizing model architectures (Sun et al., 2024; Gloeckle et al., 2024), prompt compression (Jiang et al., 2023; Pan et al., 2024), and KV cache optimization (Zhang et al., 2023; Yang et al., 2024; Hooper et al., 2024), among others. A specific approach within KV cache optimization, known as KV cache eviction, achieves efficiency improvements by exploiting characteristics and sparsity within attention mechanisms. Nevertheless, these methodologies predominantly concentrate on leveraging intrinsic sparsity of LLM itself, without considering external information to facilitate better optimization.

Previous study (Chen et al., 2021) has indicated a significant similarity in attention patterns between small and large models within the BERT architec-

ture. In Appendix A, we further substantiate that this similarity is also present in LLMs. Building upon this characteristic, this paper introduces an efficient inference technique through attention mapping between small language model (SLM) and the larger one. It is important to note that our proposed method achieves dual benefits of accelerated attention computation and reduced KV cache consumption, and is orthogonal to most existing KV cache optimization method. As depicted in Figure 1, the utilization of H_2O (Zhang et al., 2023) facilitates KV cache compression at token level, whereas our method can achieve further compression at the model’s layer level.

In this study, we investigate the methodology for achieving attention mapping between SLM and LLM while maintaining the performance of the original LLM. Initially, we evaluate the impact of various similarity metrics applied to attention matrices on language modeling efficacy. Following this, we explore how mapping at different layers of the LLM influences its language-understanding capabilities, thereby identifying the most appropriate layers for mapping. Finally, we demonstrate that the established mapping relation remains consistent throughout the inference process, enabling it to be constructed during the prefill stage and subsequently utilized in subsequent decode stage. This consistency facilitates dynamic adaptation to evolving contexts.

Based on these experiments and observations, we introduce the efficient inference through attention mapping (IAM) framework. This framework effectively captures the similarities in attention patterns between SLM and LLM to dynamically establish mapping across varying contexts. Consequently, LLM can perform efficient inference without calculating portions of attention matrices, thereby achieving dual benefits of reduced GPU memory usage for KV cache and decreased computational requirements in attention mechanisms. We first comprehensively evaluate performance preservation of IAM across four kinds of scenarios. Experimental results indicate that with a 30% mapping ratio, the model maintains performance close to lossless, while at a 50% mapping ratio, it also retains high capability levels. Efficiency evaluations across different inference scenarios demonstrate that IAM achieves an average reduction of 22.1% in KV cache usage and an average acceleration of 11% in inference speed. Our other experimental results indicate that the IAM is generalizable on

other series of LLMs and compatible with existing KV cache optimization methods.

2 Related Work

Due to the widespread adoption of technologies such as RAG and the recent emergence of reasoning models like DeepSeek-R1, the demand for handling long contexts has significantly increased. The self-attention mechanism necessitates computing attention between the current token and every preceding token, leading to the common practice of storing previous tokens’ KV states (KV cache) to avoid recomputation. However, this approach has become a primary bottleneck for managing long contexts.

One category of methods focuses on efficiently storing and transmitting large amounts of KV cache with constrained hardware. For instance, tensor parallelism (Shoeybi et al., 2020) distributes attention heads and pipeline parallelism (Huang et al., 2019) distributes attention layers across multiple GPUs, enabling horizontal scaling of KV cache storage capacity by adding more GPUs. When GPU HBM is insufficient, some techniques (Sheng et al., 2023) concentrate on efficiently offloading the KV cache to CPU memory. Mooncake (Qin et al., 2024) advances this concept further by proposing a multi-level caching strategy centered around the KV cache. At the CUDA optimization level, FlashAttention (Dao, 2023) reduces the number of read/write operations between GPU HBM and GPU cache, while PagedAttention (Kwon et al., 2023) employs virtual memory management techniques to minimize memory fragmentation in GPU HBM. These approaches primarily aim to optimize hardware capabilities and KV cache requirements from a system perspective, without addressing KV cache reduction from an algorithmic perspective.

Another category of methods focuses on leveraging the inherent similarities and sparsity within the attention mechanism. Techniques such as KVQuant (Hooper et al., 2024) exploit redundancies in numerical representations to propose quantization of the KV cache, thereby reducing storage requirements and enhancing load speeds. StreamingLLM (Xiao et al., 2024) achieves closely unlimited input by reserving both the initial and the most recent KV cache of tokens. H_2O (Zhang et al., 2023) observed that the accumulated attention scores of all tokens follow a power-law distribution, indicating that only a small subset of tokens

is highly significant in the generation. Scissorhands (Liu et al., 2023) revealed the persistence of importance, indicating that tokens identified as important in initial remain significant throughout subsequent stages of inference. PyramidInfer (Yang et al., 2024) further explores the distinct attention characteristics across different layers within LLM, and identified that deeper layers exhibit greater redundancy. These findings help design effective KV cache eviction approaches. Meanwhile, KVMerger (Wang et al., 2024) leverages the high similarity of KV states observed across different datasets to design a Gaussian kernel weighted merging algorithm for merging KV Cache, thereby minimizing the loss introduced by dropping methods. However, these approaches primarily exploit the inherent similarities and sparsity within the model’s attention mechanism and do not incorporate external information to enhance KV cache optimization, as IAM does. In addition, IAM is orthogonal to most of the aforementioned methods, due to its innovative approach of utilizing entire attention matrices of SLM and avoiding computations of attention mechanism of mapped layers in LLM.

There are also some works about speculative decoding (Xia et al., 2023; Cai et al., 2024), which employs a SLM as a draft model, followed by validation from a LLM to determine whether to adopt its predictions. Similar to our method, this approach aims to accelerate inference through the collaboration of small and large models. However, the core mechanisms differ: speculative decoding focuses on aligning the next-word prediction probability distributions between the SLM and LLM, while IAM relies on the high similarity of attention matrices between the SLM and LLM. Additionally, the LLM in speculative decoding can also benefit from the IAM method to enhance performance, achieving a synergistic effect.

3 Methodology

In this section, we begin by conducting a series of experiments aimed at providing valuable insights into attention mapping. Building on these findings, we then introduce the IAM framework.

3.1 How to Measure Similarity

A proper metric of similarity is crucial in attention mapping. It helps to capture the significant pattern within the attention matrix, thus minimizing the bias introduced by mapping in the forward process

of LLM. For vectors \mathbf{x} and \mathbf{y} , formed by flattening the lower triangular part of attention matrices of SLM and LLM, we consider the following similarity measure:

Cosine Similarity. The cosine similarity is defined as:

$$\cos \langle \mathbf{x}, \mathbf{y} \rangle = \frac{\mathbf{x} \cdot \mathbf{y}}{\|\mathbf{x}\| \|\mathbf{y}\|} \quad (1)$$

Minkowski Distance. The Minkowski Distance is defined as:

$$d(\mathbf{x}, \mathbf{y}) = \left(\sum_{i=1}^n |x_i - y_i|^p \right)^{\frac{1}{p}} \quad (2)$$

where x_i and y_i is the element in vector \mathbf{x} and \mathbf{y} , and p is the hyperparameter.

Pearson correlation. The Pearson correlation is a common measure of linear correlation between two variables. It is defined as:

$$r_{\mathbf{xy}} = \frac{\sum (x_i - \bar{x})(y_i - \bar{y})}{\sqrt{\sum (x_i - \bar{x})^2} \sqrt{\sum (y_i - \bar{y})^2}} \quad (3)$$

where x_i and y_i is the element of vector \mathbf{x} and \mathbf{y} , and \bar{x} and \bar{y} represents mean of \mathbf{x} and \mathbf{y} .

We utilize Qwen2-72B as the target LLM and consider two SLMs with different scales, Qwen2-0.5B and Qwen2-7B, as sources of attention matrices for mapping. We measure the log perplexity of the LLM on WikiText-v2 (Merity et al., 2016) after performing attention mapping using different metrics of similarity. The experimental results are presented in Table 1. It is noted that these results are obtained by dynamically matching the maximum similarity matrix between SLM and LLM during the mapping process without using a fixed mapping.

From the experimental results, it can be observed that cosine similarity achieves the best performance for both mappings from Qwen2-0.5B to Qwen2-72B and from Qwen2-7B to Qwen2-72B. Minkowski Distance with $p = 1$ also performs nearly as well as the best metric. Pearson correlation is proven unsuitable as the similarity metric due to its significantly higher perplexity. We also explore compensating the differences of the L2 norm after selecting the mapping matrix based on cosine similarity, which is named "Cosine with Norm" in Table 1. However, the experimental results indicate that this approach does not consistently and significantly enhance the performance of

Mapping	Metric	Perplexity (log)
Qwen2-0.5B to Qwen2-72B	Cosine	2.577
	Pearson	4.976
	Minkowski (p = 1)	2.589
	Minkowski (p = 2)	2.878
	Cosine with Norm	2.562
Qwen2-7B to Qwen2-72B	Cosine	2.414
	Pearson	5.376
	Minkowski (p = 1)	2.427
	Minkowski (p = 2)	2.514
	Cosine with Norm	2.421
Qwen2-72B (Original)		2.136

Table 1: The log perplexity values after conducting attention mapping using different similarity metrics. The original log perplexity is also provided in the bottom for comparison.

cosine similarity. Moreover, introducing the variable of L2 norm adds complexity to the mapping in the inference process and is unfavorable for the generalization across different contexts. Therefore, we finally choose cosine similarity as the similarity metric.

3.2 Which Layers to Map

In this section, we explore the methodology for selecting suitable layers to map, with the objective of retaining model performance. For our purposes, we utilize Qwen2-72B as the target LLM for mapping which comprises 80 transformer layers. We partitioned these layers into 10 sub-blocks (8 layers each) and make them mapped sequentially, followed by an evaluation of its performance using the MMLU benchmark.

The experimental results are shown in Figure 2. The experimental results indicate the presence of two optimal mapping regions within the Qwen2 model architecture: one situated in the final two sub-blocks (layers 64 - 80) and another located in No.2 to No.4 sub-blocks (layers 16 - 40). These regions maintain performance levels comparable to those of the original model after attention mapping. Conversely, mapping from the beginning (layers 0 - 16) is entirely impractical due to the significant performance degradation it induces.

Based on these observations, IAM adopts the following mapping strategy for Qwen2-72B: according to the user-specified mapping ratio, mappings are first performed sequentially from the last layer of the model backward to layer 64. If the specified mapping ratio is still not achieved, the

mapping continues from layer 16 onward, proceeding backwards until the requirement is met. This approach ensures a balance between maintaining model performance and achieving the desired mapping efficiency, leveraging the identified optimal regions for layer mapping.

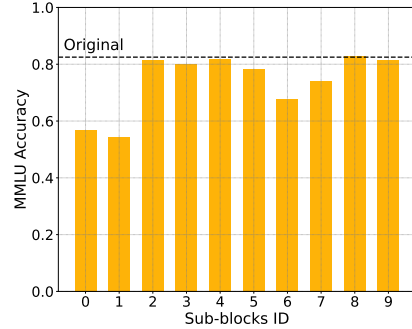


Figure 2: The performance on MMLU benchmark after mapping different attention layers of Qwen2-72B.

3.3 Consistency of Mapping

IAM establishes a mapping relationship between the SLM and the LLM based on similarity during the prefill stage, which is then utilized in the subsequent decode stage. Therefore, an essential guarantee is that the mappings established during the prefill stage remain consistent, which means mapping relationship should not significantly change as the inference progresses. To evaluate the consistency, we observe the proportion of times that the mapping does not change as consistency rate during the autoregressive generation. We also use the WikiText-v2 datasets as the prompt and set the max output tokens as 500.

The experimental results are shown in Figure 3, where we averaged the consistency rate within layers. It can be seen that a high level of consistency rate is maintained across layers. This indicates that the mapping established during the prefill stage remains stable and reliable throughout the decode stage, ensuring relatively small imprecision of mapping during the dynamic generation.

3.4 IAM Framework

Based on the preceding experiments and observations, we present the framework of IAM in this section, as shown in Figure 4. IAM initially establishes mappings during the prefill stage. Given a LLM M and a SLM M_s , the prompt is first passed through both models to obtain the attention matrices respectively. Specifically, the attention matrices of M are denoted as $A_i \in \mathbb{R}^{N \times N}$,

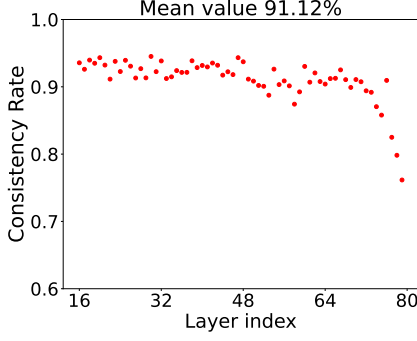


Figure 3: The average consistency rate from the 16th layer onward. A higher consistency rate indicates that the mapping established in prefill stage remains more stable and undergoes fewer changes during decoding.

332 $0 < i < L \cdot D$, and those in M_s are denoted as
 333 $A'_j \in \mathbb{R}^{N \times N}$, $0 < j < l \cdot d$. L and l represent
 334 the number of layers in the M and M_s . D and d
 335 denote the number of attention heads per layer in
 336 each model. N represents the number of tokens in
 337 the prompt. Due to differences in model architec-
 338 tures, we have $l \cdot d < L \cdot D$. And then, pairwise
 339 similarity between the attention matrices from M
 340 and M_s is computed by:

$$341 \quad S(A_i, A'_j) = \frac{\text{Tr}(A_i^T A'_j)}{\|A_i\|_F \|A'_j\|_F} \quad (4)$$

342 $\text{Tr}(\cdot)$ denotes the trace of the matrix and $\|\cdot\|_F$
 343 denotes the Frobenius norm. Finally, the mapping
 344 function is obtained by:

$$345 \quad f(i) = \arg \max_j S(A_i, A'_j) \quad (5)$$

346 In the decode stage, IAM utilizes the established
 347 mapping $f(i)$ to perform the attention mapping,
 348 which can be represented as:

$$349 \quad A_i \leftarrow A'_{f(i)} \quad (6)$$

350 Finally, the forward process of the model based
 351 on IAM can be represented as:

$$352 \quad \mathbf{Y} = M(\mathbf{X}; \theta^M, A_i \leftarrow A'_{f(i)}) \quad (7)$$

353 where \mathbf{X} and \mathbf{Y} denotes the input and output re-
 354 spectively.

355 After establishing the IAM framework, we per-
 356 form instruction tuning to mitigate the performance
 357 degradation caused by differences in the atten-
 358 tion matrices. Specifically, we utilized the Alpaca
 359 dataset (Taori et al., 2023) for this purpose. During
 360 the training process, the parameters of the large

Algorithm 1 IAM

Input: A target large language model M ; A small language model M_s ; Prompt \mathbf{x} ; Establishing threshold τ_e ; Truncation threshold τ_t ; Mapping ratio R ; Max output length L_{max} .

- 1: Calculate token length of prompt as $len(\mathbf{x})$
- 2: **if** $len(\mathbf{x}) > \tau_t$ **then**
- 3: Truncate length of prompt to τ_t
- 4: **else if** $len(\mathbf{x}) < \tau_e$ **then**
- 5: Autoregressive generation $\mathbf{y} = \{y_i\}_{i=1}^k$ by M until $len(\mathbf{x}) + k \geq \tau_e$
- 6: **end if**
- 7: Forward process by $M(\mathbf{x})$ and $M_s(\mathbf{x})$ and get attention matrices respectively
- 8: Calculate pairwise similarity via Eq.(4)
- 9: Select mapping layers according to R
- 10: Establish mapping via Eq.(5)
- 11: **while** $y_i \neq eos$ and $L < L_{max}$ **do**
- 12: Replace attention matrix of M via Eq.(6)
- 13: Autoregressive generation $\mathbf{y} = \{y_i\}_{i=k}^L$ by $M(\mathbf{x}, \mathbf{y})$
- 14: **end while**

Output: Output token sequences $\mathbf{y} = \{y_i\}_{i=1}^L$

model are frozen, and only the small model need
 to update parameters. The optimization objective
 for the M_s can be formulated as:

$$\min_{\theta^{M_s}} \mathbb{E}_{(\mathbf{X}, \mathbf{T}) \sim \mathcal{D}} \left[\mathcal{L}(M(\mathbf{X}; \theta^{M_s}, A_i \leftarrow A'_{f(i)}), \mathbf{T}) \right]$$

It is also noted that to prevent instability in the mapping established during the prefill stage due to overly short prompt, we employ a delayed establishment mechanism. This means that mapping is only initiated and performed once the number of preceding tokens N exceeds a specified threshold. Similarly, for scenarios involving long contexts, based on observations of consistency in Section 3.3, we truncate the sequences when calculating similarity to avoid inaccuracies that can arise from high-dimensional data. The detailed procedure of IAM can be referred to Algorithm 1.

4 Experiments

4.1 Experiments Setup

Datasets We comprehensively evaluate the utility preservation of IAM from four kinds of scenarios: 1) Language modeling: we measure the perplexity on WikiText-v2 (Merity et al., 2016). 2) Language understanding: We evaluate performance on

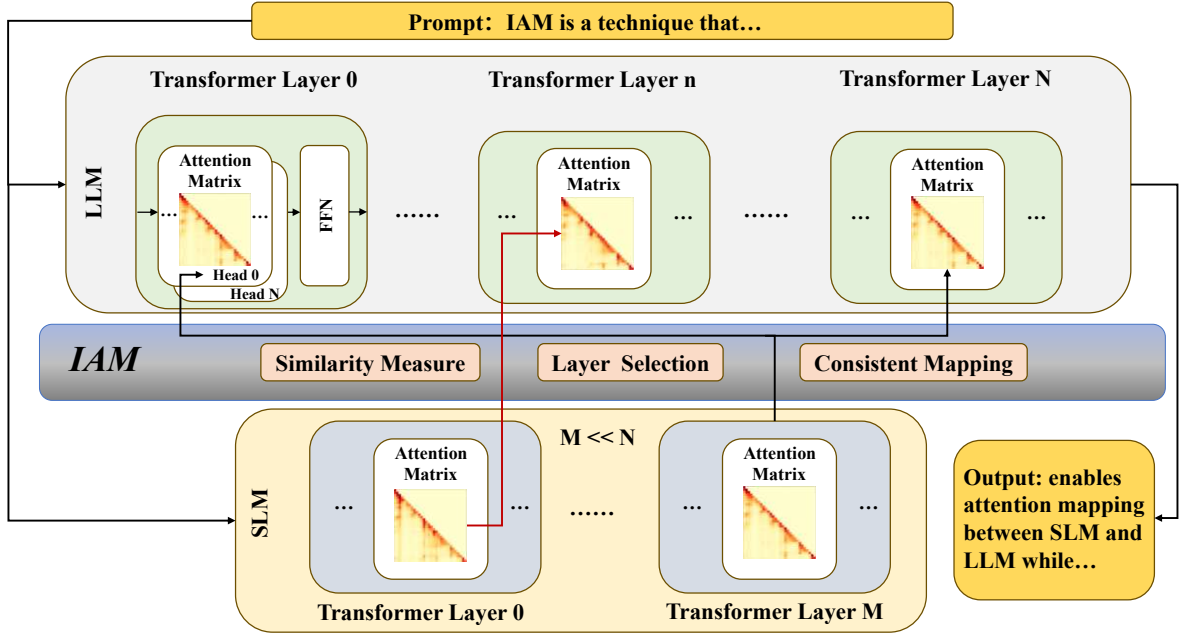


Figure 4: Framework of IAM.

the MMLU (Hendrycks et al., 2021). 3) QA task: we assess QA performance using the HotpotQA dataset (Yang et al., 2018) and adopt F1 score as evaluation metric. 4) Long context: we utilize GovReport benchmark (Huang et al., 2021) to test the long text summarization capacity.

Implementation Details Our experiments are conducted on two types of LLMs. The main results are obtained using the models of the Qwen2 series¹. Specifically, we use Qwen2-72B as target LLM and two SLMs with different scales: Qwen2-0.5B and Qwen2-7B. We also test the LLaMA3 series models² to study the IAM’s adaptation to different series LLMs in section 4.4. For these experiments, the SLM is LLaMA 3.2-1B, and the LLM is LLaMA 3.1-70B.

All experiments are performed on 8 NVIDIA A100 GPUs with . We use greedy decoding to ensure the stability of experimental results. For generative tasks, we limit the maximum output tokens to 512 and set the repetition penalty as 1.2. We also set the establishing threshold τ_e and the truncation threshold τ_t in IAM algorithm as 20 and 100 respectively. The other experimental environment includes the following configurations: CUDA version 12.0, PyTorch version 2.4.0, and

¹<https://github.com/QwenLM/Qwen>

²<https://github.com/meta-llama/llama3>

HuggingFace’s Transformers³ with version 4.45.1.

4.2 Benchmark Results

In Figure 5, we evaluate the performance of IAM in four kinds of scenarios with mapping ratio varying from 0 to 50%. It can be seen that IAM maintains high language understanding and generation quality with much less GPU memory consumption. Specifically, at a mapping ratio of 30%, IAM achieves almost the same performance as the original model. At a mapping ratio of 50%, it still retains high capability levels.

It is also important to note that using Qwen2-7B as the SLM yields better performance. We conjecture that this is because using the bigger model with more source attention matrices can improve maximum similarity between mapping layers, which will reduce the loss of mapping. This implies that there is a trade-off between efficiency and model performance.

4.3 Efficiency Analysis

To evaluate the efficiency of IAM, we consider two common scenarios: 1) Multi-user Concurrency: In this scenario, the context length is set to a prefill length of 512 tokens and a maximum generation length of 512 tokens, with a batch size of 64. 2) Long Context: In this scenario, the context length

³<https://github.com/huggingface/transformers>

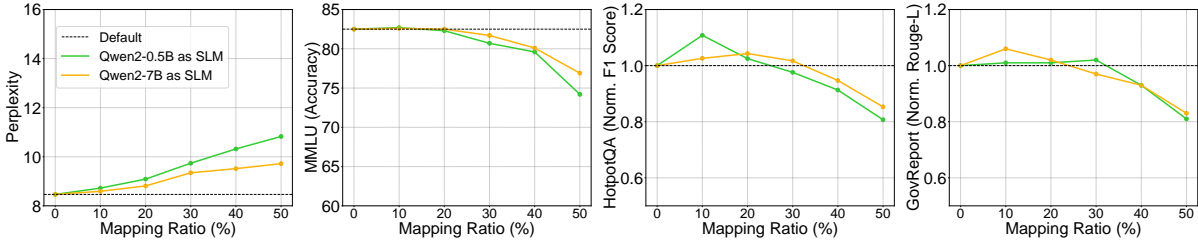


Figure 5: Benchmark results of IAM with mapping ratio varying from 0 to 50%. Default represents using the original LLM without mapping.

is set to a prefill length of 8192 tokens and a maximum generation length of 512 tokens, with a batch size of 8. In each scenario, we analyze both memory efficiency and compute efficiency, and thus derive a detailed view of the impact of IAM on end-to-end performance. The LLM used in this part of the experiment is Qwen2-72B while the SLM is Qwen2-0.5B, and the mapping ratio is set to 0.5.

Memory Efficiency With IAM, the mapped layers in the LLM do not need to store the K cache because they do not compute attention matrices. This results in a reduction of memory usage. Although the introduction of SLM with its parameters and kv cache also incurs additional overhead. It is acceptable since the SLM’s memory is significantly smaller than that of the LLM. Referring to Table 2, even when accounting for the KV cache of the SLM, IAM achieves a 21.7% reduction in KV cache usage in the multi-user concurrency scenario and a 22.5% reduction in the long context scenario, which indicates the memory efficiency of IAM.

Compute Efficiency Similarly, in IAM, the mapped layers of LLM do not need to perform Q projection, K projection, and the multiplication of the QK matrix with softmax. These computations are particularly intensive during the prefill stage and often become a performance bottleneck. By using IAM, we can significantly reduce this computational load. Although introducing the SLM adds some computational overhead, this additional workload is significantly lower compared to the computations avoided in the LLM. As a result, the overall system still sees substantial benefits: In the multi-user concurrency scenario, the reduction in computational load leads to a 12% decrease in TTFT. In the long context scenario, where the computational complexity of the QK matrix multiplication increases quadratically with sequence length, IAM provides even greater computational savings,

resulting in a more significant 17% reduction in TTFT.

End-to-end Efficiency The resulting memory and compute savings contribute to improved overall system efficiency. Benefit from the substantial reduction in K cache usage, the LLM experiences notable improvements in TPOT during the decode stage, with decreases of 11% and 10% in the multi-user concurrency and long context scenarios, respectively. Additionally, the significant reduction in computational load leads to improved TTFT during the prefill stage, with decreases of 12% and 17% in the same scenarios. These enhancements translate into improved end-to-end throughput performance. Compared to the default method, IAM achieves throughput improvements of 11% and 10% in the multi-user concurrency and long context scenarios, making it both practical and beneficial for various deployment scenarios.

4.4 Different Series Models

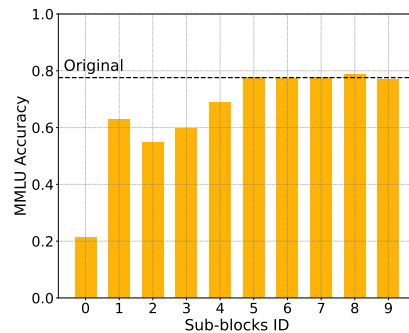


Figure 6: The performance on MMLU benchmark after mapping different attention layers of LLaMA 3.1-70B.

To evaluate the generalizability of the IAM, we conduct experiments on different series of models. In this experiment, the LLM is LLaMA 3.1-70B and the SLM is LLaMA 3.2-1B. The procedure of IAM for different series of models is largely followed the procedures detailed in the methodology

Table 2: Evaluation on efficiency of IAM. **Bsz**: batch size. **Lenth**: prefill length + decode lenth. **KV Mem.**: GPU memory usage (GB) of the KV cache. **TPOT**: average time (s) per output token in decode stage. **TTFT**: time (s) to first token. **Thr.**: End-to-end throughput (token/s)

Method	Bsz	Lenth	KV Mem.	TPOT	TTFT	Thr.
Default IAM	64	512+512	158.7 (100%) 124.2 (78.3%)	0.196 (1.0x) 0.176 (1.11x)	2.67 (1.0x) 2.39 (1.12x)	636 (1.0x) 708 (1.11x)
Default IAM	4	8192+512	187.4 (100%) 143.1 (77.5%)	0.216 (1.0x) 0.197 (1.10x)	6.72 (1.0x) 5.74 (1.17x)	297 (1.0x) 326 (1.10x)

section, with the primary modification being the re-identification of suitable layers within LLaMA 3.1-70B for mapping. Following the same approach described in Section 3.2, we test the suitable layers within LLaMA 3.1-70B and show results in Figure 8. An interesting observation is that, unlike the Qwen2 series models which exhibit two optimal mapping regions, the LLaMA series models only have a single optimal mapping region located at the end of the model. Consequently, we adjusted our mapping strategy for the LLaMA series models: as the mapping ratio increases, mappings are sequentially established from the last layer backward toward earlier layers.

After selecting the appropriate layers for mapping in the LLaMA series models, we also evaluated their performance on the MMLU benchmark under various mapping ratios. The experimental results are shown in Figure 7. Even better than the performance with the Qwen2 series, IAM demonstrates excellent language comprehension capabilities on the LLaMA series models.

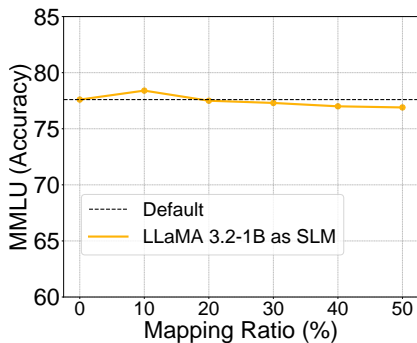


Figure 7: The MMLU benchmark results of IAM on LLaMA series models.

4.5 Compatible with KV cache compression

IAM is orthogonal to most existing KV cache compression methods due to its innovative approach of utilizing entire attention matrices of SLM for

mapping, whereas existing methods mainly focus on token-level attention importance. To illustrate this, we take H_2O (Zhang et al., 2023) as an example. In Figure 1, we demonstrate that, after the KV cache optimization of H_2O , IAM can further reduce KV cache consumption. We also evaluate the impact of using H_2O on IAM’s performance in terms of perplexity on the WikiText-v2 dataset, as shown in Figure 3. The KV cache budget of H_2O is set to 80%. Experimental results indicate that IAM is compatible with KV cache compression methods like H_2O without compromising the model’s ability of language modeling.

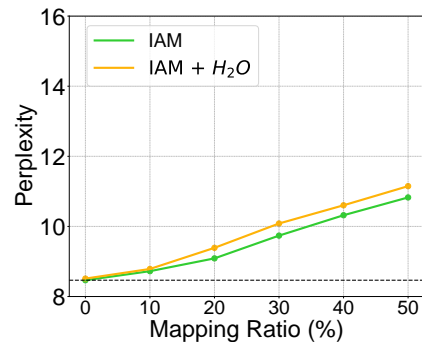


Figure 8: The perplexity of using IAM in combination with KV cache compression method H_2O .

5 Conclusion

We address the challenges faced by LLMs in serving long context scenarios by introducing IAM. This approach effectively reduces attention computation and KV cache usage by performing attention mapping between different-sized models with same series, with minimal impact on model performance. We also demonstrate that IAM is effective across different series of models. Furthermore, it is compatible with many existing KV cache optimization methods, making it a highly promising solution for deploying LLMs in resource-constrained environments.

552 Limitations

553 There are also some limitations in our approach:
554 the current analysis and implementation of IAM
555 are conducted at the granularity of model layers.
556 If the granularity is further refined to the attention
557 head, it could potentially yield additional improve-
558 ments in model performance and resource savings.
559 Additionally, IAM is not compatible with high-
560 efficiency attention methods (e.g., Flash Attention)
561 as it requires calculating attention scores. Besides
562 that, IAM can not achieve total lossless for model
563 performance.

564 References

565 Tom B Brown. 2020. Language models are few-shot
566 learners. *arXiv preprint arXiv:2005.14165*.

567 Tianle Cai, Yuhong Li, Zhengyang Geng, Hongwu
568 Peng, Jason D. Lee, Deming Chen, and Tri Dao.
569 2024. *Medusa: Simple llm inference acceleration
570 framework with multiple decoding heads. Preprint,*
571 *arXiv:2401.10774*.

572 Cheng Chen, Yichun Yin, Lifeng Shang, Xin Jiang,
573 Yujia Qin, Fengyu Wang, Zhi Wang, Xiao Chen,
574 Zhiyuan Liu, and Qun Liu. 2021. *bert2bert: To-
575 wards reusable pretrained language models. Preprint,*
576 *arXiv:2110.07143*.

577 Tri Dao. 2023. *Flashattention-2: Faster attention with
578 better parallelism and work partitioning. Preprint,*
579 *arXiv:2307.08691*.

580 DeepSeek-AI. 2025. *Deepseek-r1: Incentivizing rea-
581 soning capability in llms via reinforcement learning.*
582 *Preprint, arXiv:2501.12948*.

583 Qingxiu Dong, Lei Li, Damai Dai, Ce Zheng, Jingyuan
584 Ma, Rui Li, Heming Xia, Jingjing Xu, Zhiyong Wu,
585 Baobao Chang, et al. 2024. A survey on in-context
586 learning. In *Proceedings of the 2024 Conference on
587 Empirical Methods in Natural Language Processing,*
588 *pages 1107–1128*.

589 Fabian Gloeckle, Badr Youbi Idrissi, Baptiste Rozière,
590 David Lopez-Paz, and Gabriel Synnaeve. 2024. *Bet-
591 ter faster large language models via multi-token pre-
592 diction. Preprint, arXiv:2404.19737*.

593 Dan Hendrycks, Collin Burns, Steven Basart, Andy Zou,
594 Mantas Mazeika, Dawn Song, and Jacob Steinhardt.
595 2021. *Measuring massive multitask language under-
596 standing. Preprint, arXiv:2009.03300*.

597 Coleman Hooper, Sehoon Kim, Hiva Mohammadzadeh,
598 Michael W. Mahoney, Yakun Sophia Shao, Kurt
599 Keutzer, and Amir Gholami. 2024. *Kvquant: To-
600 wards 10 million context length llm inference with
601 kv cache quantization. Preprint, arXiv:2401.18079*.

Luyang Huang, Shuyang Cao, Nikolaus Parulian, Heng
Ji, and Lu Wang. 2021. *Efficient attentions for long
document summarization. In Proceedings of the 2021
Conference of the North American Chapter of the
Association for Computational Linguistics: Human
Language Technologies, pages 1419–1436, Online.*
Association for Computational Linguistics.

Yanping Huang, Youlong Cheng, Ankur Bapna, Orhan
Firat, Mia Xu Chen, Dehao Chen, HyookJoong Lee,
Jiquan Ngiam, Quoc V. Le, Yonghui Wu, and Zhifeng
Chen. 2019. *GPipe: efficient training of giant neural
networks using pipeline parallelism. Curran Asso-
ciates Inc., Red Hook, NY, USA.*

Huiqiang Jiang, Qianhui Wu, Chin-Yew Lin, Yuqing
Yang, and Lili Qiu. 2023. *LLMLingua: Compressing
prompts for accelerated inference of large language
models. In Proceedings of the 2023 Conference on
Empirical Methods in Natural Language Process-
ing, pages 13358–13376, Singapore. Association for
Computational Linguistics.*

Woosuk Kwon, Zhuohan Li, Siyuan Zhuang, Ying
Sheng, Lianmin Zheng, Cody Hao Yu, Joseph E.
Gonzalez, Hao Zhang, and Ion Stoica. 2023. *Ef-
ficient memory management for large language
model serving with pagedattention. Preprint,*
arXiv:2309.06180.

Patrick Lewis, Ethan Perez, Aleksandra Piktus, Fabio
Petroni, Vladimir Karpukhin, Naman Goyal, Hein-
rich Küttler, Mike Lewis, Wen-tau Yih, Tim Rock-
täschel, et al. 2020. Retrieval-augmented generation
for knowledge-intensive nlp tasks. *Advances in Neu-
ral Information Processing Systems, 33:9459–9474.*

Zichang Liu, Aditya Desai, Fangshuo Liao, Weitao
Wang, Victor Xie, Zhaozhuo Xu, Anastasios Kyril-
lidis, and Anshumali Shrivastava. 2023. *Scis-
sorhands: Exploiting the persistence of importance
hypothesis for llm kv cache compression at test time.*
*In Advances in Neural Information Processing Sys-
tems, volume 36, pages 52342–52364. Curran Asso-
ciates, Inc.*

Stephen Merity, Caiming Xiong, James Bradbury, and
Richard Socher. 2016. *Pointer sentinel mixture mod-
els. Preprint, arXiv:1609.07843*.

OpenAI. 2024a. *Gpt-4 technical report. Preprint,*
arXiv:2303.08774.

OpenAI. 2024b. *Introducing openai o1-
preview. [https://openai.com/index/
introducing-openai-o1-preview/](https://openai.com/index/introducing-openai-o1-preview/).*

Zhuoshi Pan, Qianhui Wu, Huiqiang Jiang, Menglin Xia,
Xufang Luo, Jue Zhang, Qingwei Lin, Victor Rühle,
Yuqing Yang, Chin-Yew Lin, H. Vicky Zhao, Lili Qiu,
and Dongmei Zhang. 2024. *LLMLingua-2: Data dis-
tillation for efficient and faithful task-agnostic prompt
compression. In Findings of the Association for Com-
putational Linguistics: ACL 2024, pages 963–981,
Bangkok, Thailand. Association for Computational
Linguistics.*

659	Ruoyu Qin, Zheming Li, Weiran He, Mingxing Zhang,	Shunyu Yao, Dian Yu, Jeffrey Zhao, Izhak Shafran,	714
660	Yongwei Wu, Weimin Zheng, and Xinran Xu. 2024.	Tom Griffiths, Yuan Cao, and Karthik Narasimhan.	715
661	Mooncake: A kvcache-centric disaggregated archi-	2024. Tree of thoughts: Deliberate problem solving	716
662	tecture for llm serving. <i>Preprint</i> , arXiv:2407.00079.	with large language models. <i>Advances in Neural</i>	717
		<i>Information Processing Systems</i> , 36.	718
663	Ying Sheng, Lianmin Zheng, Binhang Yuan, Zhuo-	Zhenyu Zhang, Ying Sheng, Tianyi Zhou, Tianlong	719
664	han Li, Max Ryabinin, Daniel Y. Fu, Zhiqiang Xie,	Chen, Lianmin Zheng, Ruisi Cai, Zhao Song,	720
665	Beidi Chen, Clark Barrett, Joseph E. Gonzalez, Percy	Yuandong Tian, Christopher Ré, Clark Barrett,	721
666	Liang, Christopher Ré, Ion Stoica, and Ce Zhang.	Zhangyang "Atlas" Wang, and Beidi Chen. 2023.	722
667	2023. Flexgen: High-throughput generative infer-	H2o: Heavy-hitter oracle for efficient generative in-	723
668	ference of large language models with a single gpu.	ference of large language models. In <i>Advances in</i>	724
669	<i>Preprint</i> , arXiv:2303.06865.	<i>Neural Information Processing Systems</i> , volume 36,	725
670	Mohammad Shoeybi, Mostofa Patwary, Raul Puri,	pages 34661–34710. Curran Associates, Inc.	726
671	Patrick LeGresley, Jared Casper, and Bryan Catan-		
672	zaro. 2020. Megatron-lm: Training multi-billion		
673	parameter language models using model parallelism.		
674	<i>Preprint</i> , arXiv:1909.08053.		
675	Yutao Sun, Li Dong, Yi Zhu, Shaohan Huang, Wenhui		
676	Wang, Shuming Ma, Quanlu Zhang, Jianyong Wang,		
677	and Furu Wei. 2024. You only cache once: Decoder-		
678	decoder architectures for language models. <i>arXiv</i>		
679	<i>preprint arXiv:2405.05254.</i>		
680	Rohan Taori, Ishaan Gulrajani, Tianyi Zhang, Yann		
681	Dubois, Xuechen Li, Carlos Guestrin, Percy Liang,		
682	and Tatsunori B. Hashimoto. 2023. Stanford alpaca:		
683	An instruction-following llama model. https://		
684	github.com/tatsu-lab/stanford_alpaca .		
685	Zheng Wang, Boxiao Jin, Zhongzhi Yu, and Minjia		
686	Zhang. 2024. Model tells you where to merge: Adap-		
687	tive kv cache merging for llms on long-context tasks.		
688	<i>Preprint</i> , arXiv:2407.08454.		
689	Jason Wei, Xuezhi Wang, Dale Schuurmans, Maarten		
690	Bosma, Fei Xia, Ed Chi, Quoc V Le, Denny Zhou,		
691	et al. 2022. Chain-of-thought prompting elicits rea-		
692	soning in large language models. <i>Advances in neural</i>		
693	<i>information processing systems</i> , 35:24824–24837.		
694	Heming Xia, Tao Ge, Peiyi Wang, Si-Qing Chen, Furu		
695	Wei, and Zhifang Sui. 2023. Speculative decod-		
696	ing: Exploiting speculative execution for accelerating		
697	seq2seq generation. <i>Preprint</i> , arXiv:2203.16487.		
698	Guangxuan Xiao, Yuandong Tian, Beidi Chen, Song		
699	Han, and Mike Lewis. 2024. Efficient streaming		
700	language models with attention sinks. <i>Preprint</i> ,		
701	arXiv:2309.17453.		
702	Dongjie Yang, Xiaodong Han, Yan Gao, Yao Hu, Shilin		
703	Zhang, and Hai Zhao. 2024. PyramidInfer: Pyramid		
704	KV cache compression for high-throughput LLM		
705	inference. In <i>Findings of the Association for Com-</i>		
706	<i>putational Linguistics: ACL 2024</i> , pages 3258–3270,		
707	Bangkok, Thailand. Association for Computational		
708	Linguistics.		
709	Zhilin Yang, Peng Qi, Saizheng Zhang, Yoshua Ben-		
710	gio, William W. Cohen, Ruslan Salakhutdinov, and		
711	Christopher D. Manning. 2018. Hotpotqa: A dataset		
712	for diverse, explainable multi-hop question answer-		
713	ing. <i>Preprint</i> , arXiv:1809.09600.		

A Attention Similarity between Small and Large Language Models

A fundamental premise of this paper is the high similarity of attention matrices across different-sized models within same series. We first demonstrate the visualization of average attention matrices across all layers and all heads under a given context in WikiText-v2 using four different-size models from the Qwen2 series, as shown in Figure 11. It can be observed that these matrices exhibit strong similarities in their attention patterns.

We also provide a quantitative analysis of this similarity. Considering the WikiText-v2 dataset, we use the SLM of Qwen2-7B and the LLM of Qwen2-72B to compute the average cosine similarity of all pairwise most similar matrices. The result yield a average cosine similarity of 0.954. For comparison, we also test the case where the SLM is llama3.2-1B. Due to the difference of tokenizers, we employ the pairwise longest common subsequence method to align tokens between the two models. In this situation, the average cosine similarity is 0.568.

B Detailed Analysis of Mapping Strategy

In Section 3.2, we present a mapping strategy from a practical perspective, specifically by using benchmark scores to determine which layers are most suitable for mapping. In this section, we provide additional analysis of the mapping strategy. There is a natural consideration of mapping the layers with the highest average cosine similarity, aiming to minimize the loss introduced by mapping. To this end, we first calculate the average cosine similarity for each layer of Qwen2-72B, as shown in Figure 9. It is evident that the layers in the first half of the model, excluding the first two layers, exhibit more strong similarity.

We consider three mapping strategies: From the Front-End (mapping only the initial layers), From the Back-End (mapping only the latter layers), and the Most Similar (mapping the layers with the highest mean cosine similarity). Using the same evaluation methodology as described in section 3.1, the experimental results are illustrated in Figure 10, where the x-axis represents the percentage of layers mapped relative to the total number of layers. From experimental results, it is evident that the From the Front-End strategy is entirely unviable. The From the Back-End strategy yields the best results, even outperforming the Most Similar approach. We con-

jecture that this can be attributed to the cumulative error introduced by front-end mapping, which progressively accumulates through each subsequent layer. Consequently, introducing mappings at the back-end leads to fewer alterations from the original model, thereby maintaining a relatively greater capability of the LLM. This also explains why mapping the latter layers consistently yields better performance, both in the Qwen2 series models and the LLaMA3 series models.

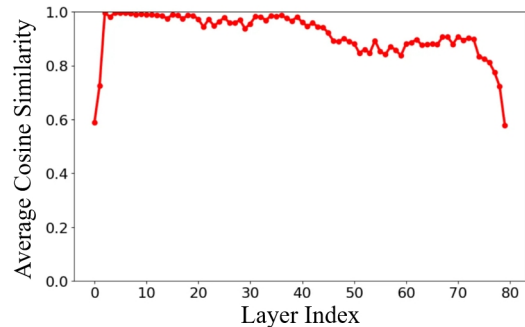


Figure 9: The average cosine similarity for each layer of Qwen2-72B by calculating the most similar attention matrix between Qwen2-7B and Qwen2-72B.

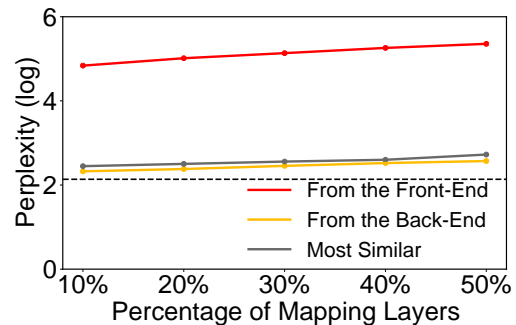


Figure 10: The log perplexity of LLM according to different mapping layer selecting strategies.

C Statistical Analysis of Mapping Relations

We also conduct a statistical analysis of the most frequent mapping relations on the WikiText-v2 dataset. Specifically, we record the mapping relations for each context. For each attention head of the LLM, we identify the mode of its mapping index. In this experiment, we used a SLM of Qwen2-0.5B and a LLM of Qwen2-72B, resulting in a mapping from 5120 to 360. The experimental results are shown in Figure 12.

Firstly, it can be observed that most matrices from the SLM are utilized in the mapping process,

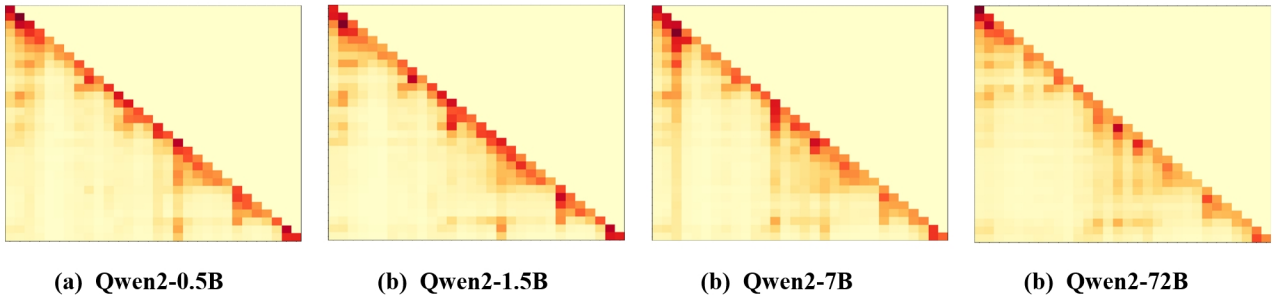


Figure 11: The average attention matrices across all layers and all heads from four different-size models of Qwen2 series

800 with the exception of the first forty matrices, which
 801 are rarely used. Additionally, the mapping relations
 802 exhibit a strong imbalance across different matri-
 803 ces. The most frequently used matrix is utilized
 804 over 1200 times, significantly more than any other
 805 matrix. This finding suggests that the attention
 806 matrices within the LLM might have substantial
 807 sparsity.

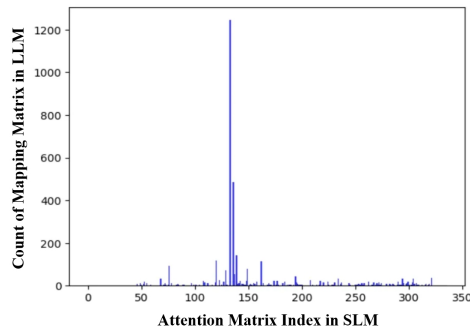


Figure 12: The statistical analysis of the most frequent mapping relations between Qwen2-0.5B and Qwen2-72B.